

oml

RECEIVED

ORNL/TM-12675

MAR 13 1996

OSTI

**OAK RIDGE
NATIONAL
LABORATORY**

MARTIN MARIETTA

**The FALSTF Last-Flight Computer
Program**

R. L. Childs

**MANAGED BY
MARTIN MARIETTA ENERGY SYSTEMS, INC.
FOR THE UNITED STATES
DEPARTMENT OF ENERGY**

DISTRIBUTION OF THIS DOCUMENT IS UNLIMITED
DRC

This report has been reproduced directly from the best available copy.

Available to DOE and DOE contractors from the Office of Scientific and Technical Information, P.O. Box 62, Oak Ridge, TN 37831; prices available from (615) 576-8401, FTS 626-8401.

Available to the public from the National Technical Information Service, U.S. Department of Commerce, 5285 Port Royal Rd., Springfield, VA 22161.

This report was prepared as an account of work sponsored by an agency of the United States Government. Neither the United States Government nor any agency thereof, nor any of their employees, makes any warranty, express or implied, or assumes any legal liability or responsibility for the accuracy, completeness, or usefulness of any information, apparatus, product, or process disclosed, or represents that its use would not infringe privately owned rights. Reference herein to any specific commercial product, process, or service by trade name, trademark, manufacturer, or otherwise, does not necessarily constitute or imply its endorsement, recommendation, or favoring by the United States Government or any agency thereof. The views and opinions of authors expressed herein do not necessarily state or reflect those of the United States Government or any agency thereof.

Computational Physics and Engineering Division

THE FALSTF LAST-FLIGHT COMPUTER PROGRAM

R. L. Childs

Date Published: January 1996

Prepared by the
Oak Ridge National Laboratory
Oak Ridge, Tennessee 37831-6370
managed by
LOCKHEED MARTIN ENERGY RESEARCH CORP.
for the
U.S. DEPARTMENT OF ENERGY
under contract DE-AC05-96OR22464

MASTER



CONTENTS

	<u>Page</u>
LIST OF FIGURES	iv
LIST OF TABLES	v
ABSTRACT	vii
1. INTRODUCTION	1
2. THEORY	3
3. DORT REQUIREMENTS	6
4. FALSTF INPUT DATA	7
5. R-Z SAMPLE PROBLEM	8
6. R- θ SAMPLE PROBLEM	14
7. REFERENCES	16
APPENDIX A. THE VARSOR2D INTERFACE FILE	17
APPENDIX B. THE R-Z SAMPLE PROBLEM FALSTF OUTPUT	21

LIST OF FIGURES

<u>Figure</u>		<u>Page</u>
1	Geometry of problem 1a cast-iron cask specified by OECD Working Group	9
2	CSASI input to generate cross sections	10
3	SAS4 input used to compare with FALSTF	12
4	The R- θ sample problem geometry	15
5	Dose at 1 m from the surface	15

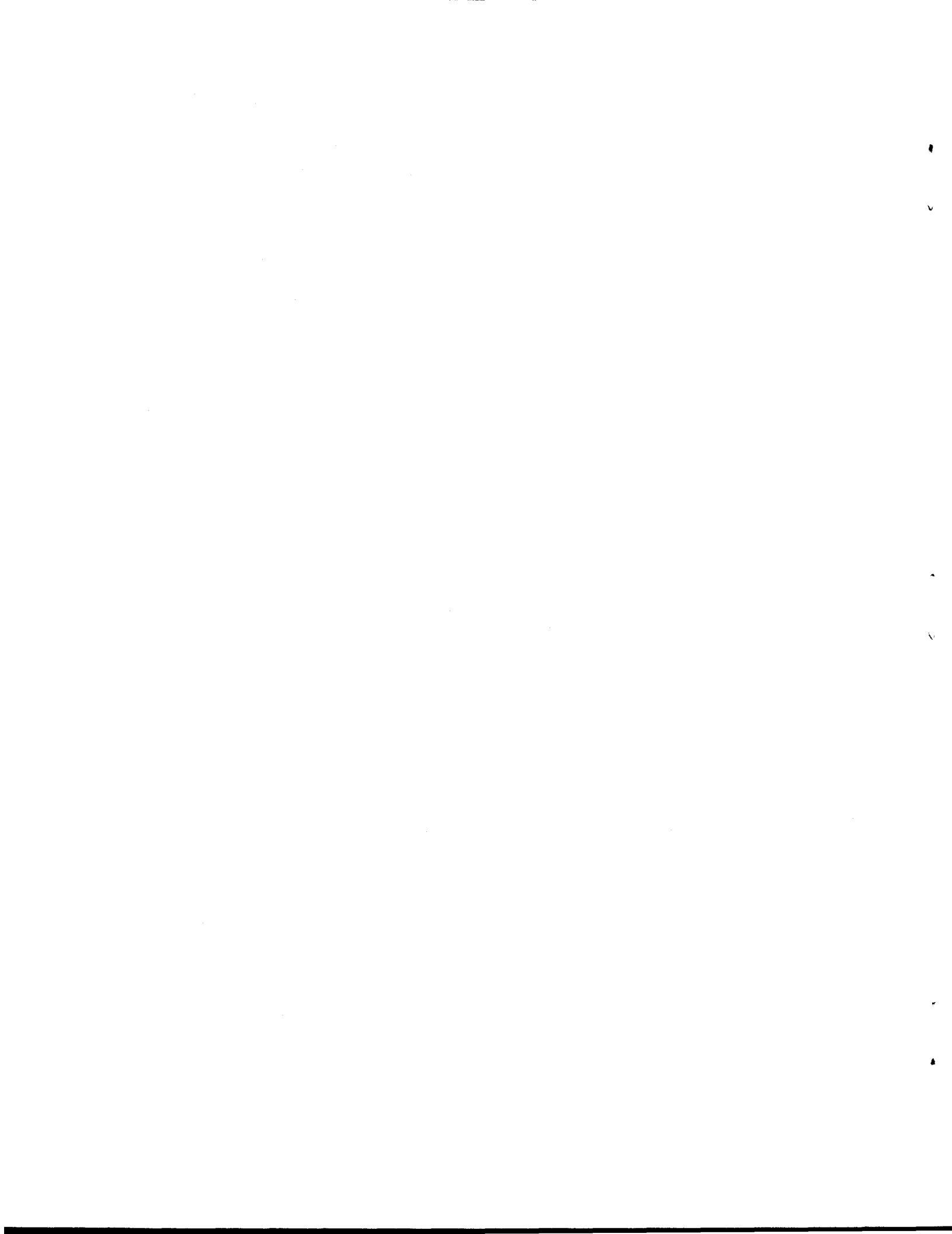
LIST OF TABLES

<u>Table</u>		<u>Page</u>
1	Groupwise gamma source	10
2	FALSTF calculated dose at 2 m above the lid from FALSTF vs mesh size	11
3	Dose in $\mu\text{Sv/h}$ at 0.4 m off centerline vs NOA	11
4	Centerline doses ($\mu\text{Sv/h}$) from FALSTF and SAS4 vs distance above lid	12
5	Doses ($\mu\text{Sv/h}$) radially averaged over cavity area from FALSTF and SAS4 vs distance	13



ABSTRACT

FALSTF is a computer program used with the DORT transport code to calculate fluxes and doses at detector points located outside the DORT geometry model. An integral form of the transport equation is solved to obtain the flux at the detector points resulting from the uncollided transport of the emergent particle density within the geometry as calculated by DORT. Both R-Z and R- θ geometries are supported.



1 INTRODUCTION

FALSTF is a computer program used in conjunction with the DORT¹ discrete-ordinates transport code to calculate dose rates and group fluxes at point detector locations specified by the user. R-Z and R- θ cylindrical geometries are allowed. Mynatt² developed the theoretical basis for FALSTF using a last-flight importance function. Next-event estimation used in Monte Carlo programs to calculate an effect of interest at point detectors is based upon the same principle. Bell and Glasstone³ derived an equation for the energy-dependent flux at a point by integrating the integral form of the transport equation over direction. Equation (1.29) of ref. 3 is the equation that is evaluated numerically by FALSTF for the isotropic scattering case.

The basic concept used by FALSTF is that the transport from the last collision site to the detector is done analytically rather than by using the method of discrete ordinates. This treatment gives a more accurate answer when the discrete-ordinates method is subject to ray effects or when the angular quadrature used in DORT does not have enough angles to give adequate angular resolution. The usual application of FALSTF is for detectors located in a void outside the DORT geometry. For example, FALSTF is quite useful for determining the dose 2 m from the surface of a cylindrical waste package or spent fuel package. FALSTF detectors can also be placed inside the DORT geometry. Detectors inside a DORT geometry containing a large cavity can sometimes be calculated more accurately with FALSTF than with DORT.

Difficulties calculating the dose 30 m from space reactor shields with existing methods was the motivating factor for the development of the original R-Z geometry FALSTF in 1971. Since then, FALSTF has been used (primarily at ORNL) for a number of applications, including the analysis of shielding experiments performed at the Tower Shielding Facility. These experiments included measurements of gamma-ray spectra more than 10 m from the shield configurations and neutron spectra more than 3 m away.

Several difficulties can arise in the use of the original FALSTF. Perhaps the most serious limitation is that the newer geometry input methods available in DORT, including zone specification by overlay, are not available. Also, valid DORT cross-section mixing table input can cause incorrect answers because the original FALSTF uses the obsolete requirements of DOT III. To overcome these difficulties, FALSTF has been modified extensively to provide the code described in this report. The amount of input required has been reduced substantially by reading most of the required information from the interface file written by DORT and by removing several options deemed unlikely to be needed. The new input specifications make the preparation and checking of FALSTF input much easier and reduce the danger of incorrect results. An R- θ geometry option has also been added.

A principal motivation for updating the original FALSTF code and adding the R- θ option originated from a calculation benchmark effort completed in 1992. Within the Organization for Economic Cooperation and Development (OECD), the Nuclear Energy Agency Committee on Reactor Physics set up a working group on the shielding assessment of spent fuel transportation packages in 1985.^{4,5} Six theoretical benchmark problems were studied by participants from 12 countries. The methods used for dose calculations included one-dimensional (1-D) and two-dimensional (2-D) discrete-ordinates, point and multigroup Monte Carlo, and kernel methods. The U.S. contribution to this study included DORT/FALSTF calculations and SAS4/MORSE⁶ multigroup Monte Carlo calculations. The doses calculated using DORT and FALSTF agreed quite

well with those obtained from SAS4. The agreement with point Monte Carlo results was also good. Other 2-D discrete-ordinates solutions to the benchmark problems that extended the problem mesh to include the dose points had difficulties with ray effects. These problems were particularly prominent for top and bottom doses.

An alternative to the FALSTF approach is to perform a surface integration to obtain the dose at detectors in a void beyond the surface. This alternative approach was investigated, but the results discussed in Sect. 6 indicated that the method is not as accurate as the FALSTF methodology. Also, the boundary angular flux from a discrete-ordinates calculation used in the surface integration method does not provide as much information about the angular variation of the leakage flux as the volume integration method applied by FALSTF.

2 THEORY

In (R, θ, Z) cylindrical coordinates, the group flux at a detector point is

$$\phi_{\text{det}} = \int_0^R \int_0^{2\pi} \int_{Z_B}^{Z_T} \frac{S_D(r, \theta, Z) e^{-\lambda_D(r, \theta, Z)}}{4\pi[\rho_D(r, \theta, Z)]^2} r dr d\theta dZ. \quad (1)$$

ϕ_{det} is the scalar flux at the detector point for the group.

R is the outside radius of the cylinder (a void is assumed at points outside the cylinder).

Z_B and Z_T are the bottom and top Z coordinates of the cylinder.

$S_D(r, \theta, Z)/4\pi$ is the total source per unit volume per steradian at point (r, θ, Z) in the direction of the detector. The total source includes the distributed source, the fission source, and all scattering sources (downscatter, within-group scatter, and upscatter).

$\lambda_D(r, \theta, Z)$ is the distance from point (r, θ, Z) to the detector point measured in mean-free paths for the group. In FALSTF, λ_D is calculated by summing the product of the distance traveled in each material and the total cross section for the material.

$\rho_D(r, \theta, Z)$ is the distance from point (r, θ, Z) to the detector point.

In order to perform the volume integration in Eq. (1) in a 2-D, R - Z geometry, it is assumed that the source in each DORT mesh cell is a circular line source located at the radial and axial midpoint of the mesh cell. The volume integration is thus replaced by an integral over the variable θ . Since DORT(R, Z) problems have azimuthal symmetry, the azimuthal location of the detector can be defined to be zero, and $\int_0^{2\pi} d\theta$ may be replaced with $2 \int_0^\pi d\theta$. This integration is performed with a numerical quadrature.

The contribution of the source in each mesh cell is thus evaluated by summing the contribution of noa point sources, where noa is the number of terms used in the numerical quadrature.

The contribution to ϕ_{det} from a point source located at $(\bar{r}, \theta_n, \bar{Z})$ is

$$\begin{aligned} \phi_p &= \frac{S_D e^{-\lambda_D}}{4\pi \rho_D} \bar{r} \Delta r (2\pi W_n) \Delta Z \\ &= \frac{\bar{r} \Delta r \Delta Z}{2} \frac{S_D e^{-\lambda_D}}{\rho_D} W_n, \end{aligned} \quad (2)$$

where

\bar{r} is the radial midpoint of the mesh cell,

Δr is the radial thickness of the mesh cell,

\bar{Z} is the axial midpoint of the mesh cell,

ΔZ is the axial thickness of the mesh cell,

θ_n is the n th θ location used in the quadrature integration $0 \leq \theta \leq \pi$,

W_n is the n th weight for the quadrature integration $\left(\sum_{n=1}^{\text{NOA}} W_n = 1 \right)$,

S_D is the total source per unit volume per unit sphere in the direction from the point source to the point detector located at $(r_{\text{det}}, 0, Z_{\text{det}})$,

λ_D is the distance from the point source to the point detector measured in mean-free paths (a ray-tracing calculation is used to determine λ_D),

ρ_D is the distance from the point source to the point detector.

The value of S_D is obtained using the same spherical harmonics expansion used by DORT to obtain directional sources for the discrete-ordinates calculation:

$$S_D = \sum_{\ell=0}^L \sum_{m=0}^{\ell} \sqrt{(2 - \delta_{0,m}) \frac{(\ell - m)!}{(\ell + m)!}} P_{\ell}^m(\mu_D) \cos(m\psi) S_{\ell}^m, \quad (3)$$

where

μ_D is the cosine of the angle between the vector, \vec{v}_r , from $(0, 0, \bar{Z})$ to $(\bar{r}, \theta_n, \bar{Z})$ and the vector, \vec{v}_D , from $(\bar{r}, \theta_n, \bar{Z})$ to $(r_{\text{det}}, 0, Z_{\text{det}})$;

ψ is the angle between the projection of vector \vec{v}_D onto the plane perpendicular to \vec{v}_r and the Z axis;

S_{ℓ}^m are source moments read directly from the interface file written by DORT.

Replacing the volume-distributed source for an interval with a line source can produce incorrect results when a detector is placed in or near a mesh cell that contains a source. The fact that $1/\rho_D^2$ in Eq. (1) is a rapidly varying function of space makes the approximation invalid. FALSTF is typically used for detectors outside the DORT geometry where ρ_D is much greater than the radial or axial thickness of any mesh cell.

In R- θ geometry, it is assumed that the source in each DORT mesh cell is a line source located at the radial and θ midpoint of the mesh cell. The volume integration of Eq. (1) is replaced by an integral over the variable Z . This integration is performed with a numerical quadrature. Also, the θ integration from 0 to 2π must be performed even when the DORT geometry covers only part of the angular range (a 45° segment for example). Either periodic or reflected θ boundary conditions are used to extend the angular range to 2π .

Equation (3) for the source in the direction of the detector is also used in R- θ cases, but the angle ψ is measured relative to a vector in the $+\theta$ direction; in the R- Z case ψ is measured relative to a vector in the $+Z$ direction.

3. DORT REQUIREMENTS

DORT Version 2.10.2 or later must be used with FALSTF. Beginning with this version, unit *ntdso* is written in *varsor2d* format. This new interface format is described in Appendix A. The interface file written on unit *ntdso* provides FALSTF with most of the information needed to calculate the dose at each detector point, such as the mesh description, the zone map, and the total cross section for each group and material. DORT Version 2.12.14 was given to the Radiation Shielding Information Center (RSIC) in December 1994.

When DORT R-Z geometry (*inggeom* = 1) is used, the radial mesh should start at zero. The left boundary should be reflected (*ibl* = 1), and the right boundary condition should be void (*ibr* = 0). The top and bottom boundary conditions should both be void (*ibb* = *ibt* = 0). When the bottom boundary is reflected, correct results for detectors located at the same axial location as the bottom boundary can be obtained by doubling the result.

When DORT R- θ geometry (*inggeom* = 2) is used, the left boundary condition should be void or reflected (*ibl* = 0 or 1), and the right boundary condition should be void (*ibr* = 0). The left boundary condition must be void (no entering particles) if the radial mesh does not start at zero radius. The top boundary condition should be reflected or periodic (*ibt* = 1 or 2), and the bottom boundary condition should be the same as the top boundary condition. The θ mesh should span $360/n$ degrees, where n is a positive integer for a periodic top boundary condition and an even positive integer for a reflected top boundary condition.

FALSTF does not allow density factors (*idfac* = 1). Most problems can be modeled without density factors. This option could be added in the future if the need arises.

If boundary sources (either internal or external) are used, FALSTF results will not include the uncollided contribution from these sources. First collision source problems will not include the uncollided contribution.

Variable mesh (*im* < 0) is allowed for R- θ geometry (*inggeom* = 2) but not for R-Z geometry (*inggeom* = 1). Many R-Z problems (such as spent fuel packages) can be modeled without variable mesh. Variable mesh could be added in the future.

4. FALSTF INPUT DATA

Because most of the information needed by FALSTF is read from an interface file, the input required is quite short. Two data blocks are entered using FIDO input. Optional title cards may be read after the FIDO input.

Block 1.

1\$ Logical Assignments (3 entries)

1. *ntdso* - DORT distributed source unit (default = 30)
2. *ntf* - output unit for detector flux (default = 0)
0 means no file written
3. *ntzf* - output unit for detector flux contribution by zone
(default = 0) 0 means no file written

2\$ Integer Input Variables

1. *ndet* - number of detector locations (default = 1)
2. *neut* - last neutron group; 0 means only gamma groups
(default read from *ntdso*)
3. *noa* - number of angles for the azimuthal integration in R-Z geometry (default = 12)
or
number of Z points for the axial integration in R- θ geometry

T Terminate Block 1.

Block 2.

- 26* dose multiplier by detector (*ndet* entries) default = 1.0
27* dose factor by group (*igm* entries, *igm* is the number of groups) default = 1.0
34* Z limits for the axial integration in R- θ geometry (two entries, R- θ geometry only)
42* detector radial locations (*ndet* entries)
43* detector θ locations (*ndet* entries, R- θ geometry only)
44* detector axial locations (*ndet* entries)

T Terminate Block 2.

From zero to ten title cards may be entered here. The first 72 characters are printed in the output.

FALSTF calculates neutron dose and gamma dose using the dose factors supplied in the 27* array. The variable *neut* is used to determine which groups are neutron groups. The dose is multiplied by the factors from the 26* array. Group fluxes are written in a text file on unit *ntf* when *ntf* is not zero. A text file containing group fluxes at the detector points resulting from sources in

each zone of the geometry are written on unit *ntzf* when *ntzf* is nonzero. Summing the numbers from *ntzf* over zone gives the numbers on *ntf*.

The input parameter *noa* specifies how the azimuthal or axial integration is performed. If the input value of *noa* is not a multiple of 6, the value of *noa* is modified to make it a multiple of 6. If *noa* is 6, an S_6 Gaussian quadrature is used to perform the integration from 0 to π for R-Z geometry. If *noa* is 12, two separate integrations, one from 0 to $\pi/2$ and one from $\pi/2$ to π , are each performed with an S_6 Gaussian quadrature. In general, the integration is broken up into $noa/6$ equal intervals, and each of these intervals is integrated with the S_6 Gaussian quadrature. For R- θ geometry, the integration is from Z_B to Z_T , which are entered in the 34* array.

5. R-Z SAMPLE PROBLEM

The R-Z sample problem is the OECD problem 1a taken from the benchmark set discussed in Sect. 1.^{4,5} Only the lid detectors are analyzed. The geometry is shown in Fig. 1. The radius of the steel lid is 40 cm in the model used for these calculations. Only the top 72 cm of the spent fuel region was included in the model. Truncating the model at this point reduces the calculated lid doses by less than 1%, while allowing a very fine mesh case to be run to study the effect of mesh size on the calculated dose. The SCALE⁷ 27-18 group-structure is used. The input for the CSASI⁷ case used to generate the cross sections is shown in Fig. 2. The source for the sample problem is shown in Table 1. This source is the fission-product source for OECD problem 1a from ref. 4.

Table 2 shows the effect of varying the mesh size on the centerline dose 2 m above the lid. Uniform meshes with equal radial and axial mesh sizes were used. The error in the calculation is reduced by roughly a factor of 4 each time the mesh size is halved. This indicates that the error is second order. It is seen that a mesh size of 0.5 cm has an error of 1.3%.

Table 3 shows the effect of varying the input parameter *noa* that controls the azimuthal integration. The detectors are at a radius of 40 cm. The 0.5-cm mesh case was used for these calculations. Only the detector very near the surface requires a value of *noa* larger than the default value of 12 to obtain accurate results. In most cases, the dose this close to the surface should be obtained directly from DORT without using FALSTF.

The input for a SAS4 case with 6000 batches and 4000 particles per batch is shown in Fig. 3. The fraction standard deviation was about 1.5% for each detector. Table 4 compares centerline point detector results from SAS4 with FALSTF results using the 0.25-cm mesh. The agreement is quite good at 1 m but progressively worsens with increasing distance from the surface. Table 5 compares boundary crossing estimators from SAS4 that are averaged over the area of the cavity (0 to 40 cm) with FALSTF results. The FALSTF results were obtained by placing point detectors every 4 cm from 0 to 40 cm and by performing a numerical integration. The SAS4 result was about 5% higher than the FALSTF result at 1 m.

A FALSTF output is shown in Appendix B. The number of groups is 13 for this case. The top five groups in the 18 gamma-ray group structure were deleted in the DORT calculation since there is no source in these groups. The case shown has a 2-cm mesh.

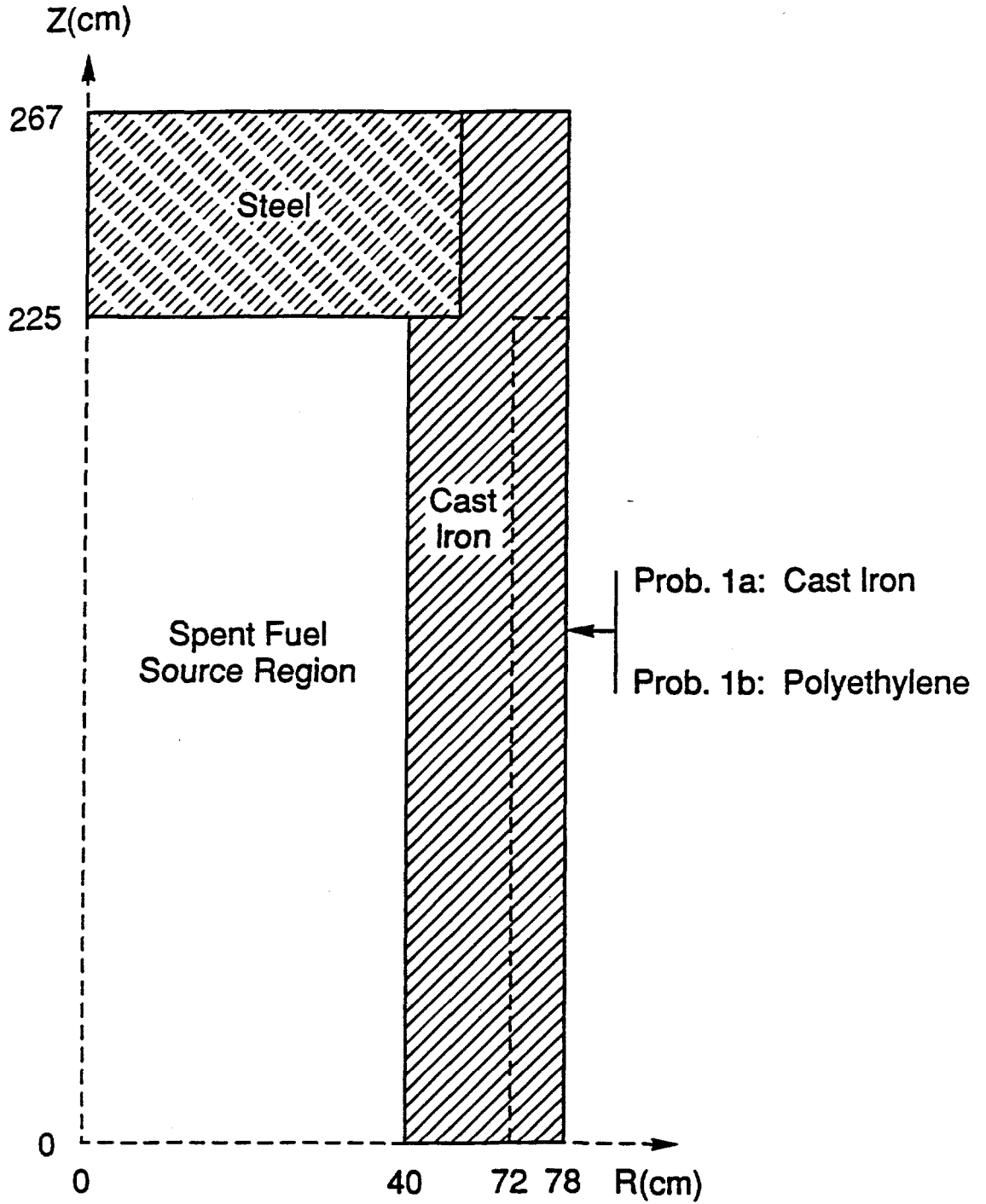


Fig. 1. Geometry of problem 1 cast-iron cask specified by OECD Working Group.

```

=csasi
case la-4, top primary gamma dose, dry fuel
27n-18couple infhommedium
arbm-1.4313 7.7 4 0 0 1 25055 1.5 24000 12.5 28000 4.0 26000 82. 1 end
arbm-castfe 7.0 4 0 0 1 6012 3.25 14000 1.4 28000 1.1 26000 94.25 2 end
arbm-zirc4 2.81 3 0 0 1 40000 97.9 50000 1.6 26000 0.5 3 .116 end
arbm-u235 2.81 1 0 0 1 92235 100. 3 .011 end
arbm-u238 2.81 1 0 0 1 92238 100. 3 .344 end
arbm-oxygen 2.81 1 0 0 0 8016 100. 3 .043 end
arbm-1.4541 2.81 4 0 0 1 25055 2. 24000 18. 28000 10. 26000 70. 3
      .186 end
end comp
end
=alpo
-1$$ 27 1452 1 f0
0$$ 60 0
1$$ 1 3 4 48 3 3z t
2$$ 2 0 t
end

```

Fig. 2. CSASI input to generate cross sections.

Table 1. Groupwise gamma source

Gamma group No.	Total gamma source (particles/s)
1	0
2	0
3	0
4	0
5	0
6	1.344×10^{12}
7	2.547×10^{14}
8	5.713×10^{12}
9	0
10	9.120×10^{14}
11	3.861×10^{14}
12	3.404×10^{16}
13	1.518×10^{16}
14	0
15	0
16	0
17	0
18	0

Table 2. FALSTF-calculated dose at 2 m above the lid vs mesh size

Mesh size (cm)	Dose ($\mu\text{Sv/h}$)	Percent error
2	4.351	-19.0
1	5.089	-5.2
0.5	5.297	-1.3
0.25	5.351	-0.3
Extrapolated	5.369	

Table 3. Dose in $\mu\text{Sv/h}$ at 0.4 m off centerline vs *noa*

<i>noa</i>	Distance above lid			
	0.005 m	1.0 m	2.0 m	10.0 m
6	19.18	11.02	4.738	0.2838
12	27.07	11.02	4.739	0.2838
18	29.60	11.02	4.738	0.2837
24	30.58	11.02	4.739	0.2837
30	31.00	11.02	4.738	0.2837
36	31.14	11.02	4.738	0.2837

```

=sas4
case 1a-4, top primary gamma dose, dry fuel
27n-18couple infhommedium
arbm-1.4313 7.7 4 0 0 1 25055 1.5 24000 12.5 28000 4.0 26000 82. 1 end
arbm-castfe 7.0 4 0 0 1 6012 3.25 14000 1.4 28000 1.1 26000 94.25 2 end
poly(h2o) 3 0.98913 end
arbm-zirc4 2.81 3 0 0 1 40000 97.9 50000 1.6 26000 0.5 4 .116 end
arbm-u235 2.81 1 0 0 1 92235 100. 4 .011 end
arbm-u238 2.81 1 0 0 1 92238 100. 4 .344 end
arbm-oxygen 2.81 1 0 0 0 8016 100. 4 .043 end
arbm-1.4541 2.81 4 0 0 1 25055 2. 24000 18. 28000 10. 26000 70. 4
      .186 end
c 5 0.0 1.00-20 end
c 6 0.0 1.00-20 end
end comp
ity=2 idr=1 szf=2 izm=2 mhw=6 frd=39.99 ifs=1 end
225. 267. end
4 1 end
xend
tim=800. sfa=5+16 nst=4000 nmt=6000 nit=6000 nod=3 igo=0 nco=8
fr2=.285714 fr3=.285714 fr4=.285714 end
soe 32z 1.344+12 2.547+14 5.713+12 0 9.12+14 3.861+14 3.404+16
      1.518+16 5z end
det 2z 367 2z 467 2z 1267 end
gend
case 1a-4, top geometry
fue 224.98 224.99 end
fend
cav 6 40. 225. end
inn 6 40.01 225.01 end
rs1 2 78. 267. end
as1 1 40.01 267. end
our 6 78.01 267.01 end
cend
end

```

Fig. 3. SAS4 input used to compare with FALSTF.

Table 4. Centerline doses ($\mu\text{Sv/h}$) from FALSTF and SAS4 vs distance above lid

Distance above lid (m)	FALSTF	SAS4	FALSTF/SAS4
1	14.51	14.76	0.983
2	5.35	5.59	0.957
10	0.288	0.320	0.900

Table 5. Doses ($\mu\text{Sv/h}$) radially averaged over cavity area
from FALSTF and SAS4 vs distance

Distance above lid (m)	FALSTF	SAS4	FALSTF/SAS4
1	12.79	13.42	0.953
2	5.08	5.51	0.922
3	2.63	2.86	0.919

6. R- θ SAMPLE PROBLEM

The DORT geometry for the R- θ sample problem is shown in Fig. 4. This shipping cask problem includes the following materials radially: fuel, SS304, aluminum, SS304, lead, concrete, SS304. The SCALE 27-18 group structure is used, but only the gamma dose is calculated. A sample FALSTF input for this case is the following:

```

2$$ 46 27 24 e
t
26** f2
27**
1.4916-4 1.4464-4 1.2701-4 1.2811-4 1.2977-4 1.0281-4
5.1183-5 1.2319-5 3.8365-6 3.7247-6 4.0150-6 4.2926-6
4.4744-6 4.5676-6 4.5581-6 4.5185-6 4.4879-6 4.4665-6
4.4345-6 4.3271-6 4.1975-6 4.0976-6 3.8390-6 3.6748-6
3.6748-6 3.6748-6 3.6748-6
8.7716-6 7.4785-6 6.3748-6 5.4136-6 4.6221-6 3.9596-6
3.4686-6 3.0192-6 2.6276-6 2.2051-6 1.8326-6 1.5228-6
1.1725-6 8.7594-7 6.3061-7 3.8338-7 2.6693-7 9.3472-7
34** 0 182.88
42** 46r200.647
43** 44i0 .125
44** f0
t

```

This input indicates that all of the detectors are located at a Z of zero and the axial integration is from 0 to 182.88. The 2 in the 26* array indicates that the doses are multiplied by 2, which gives the result for an integration from -182.88 to 182.88 (the full height of the fuel).

Figure 5 shows the dose distribution at 1 m from the surface of a spent fuel shipping cask obtained by three different methods. All three methods use the same DORT calculation of the cask. The solid curve was obtained by extending the DORT mesh and by getting the dose values directly from DORT. The dashed curve was obtained using FALSTF. The dotted curve was obtained from a surface-integration method. The areas under the three curves differ by less than 3%. This small difference indicates that the azimuthally averaged dose is about the same for all three cases even though the calculated angular distributions are very different. The DORT result is not as smooth as the other two results and has a higher peak value and a lower minimum value. The DORT and surface-integration results have local maxima near 20 and 40° and a local minimum near 30°. The peaks appear to be ray effects resulting from the discrete angles in the angular quadrature. The FALSTF result has a maximum near 25°, which is where the surface peak dose occurs. Thus the FALSTF result is believed to be the best of the three, due primarily to the physical nature of the solution since experimental or Monte Carlo results are not available.

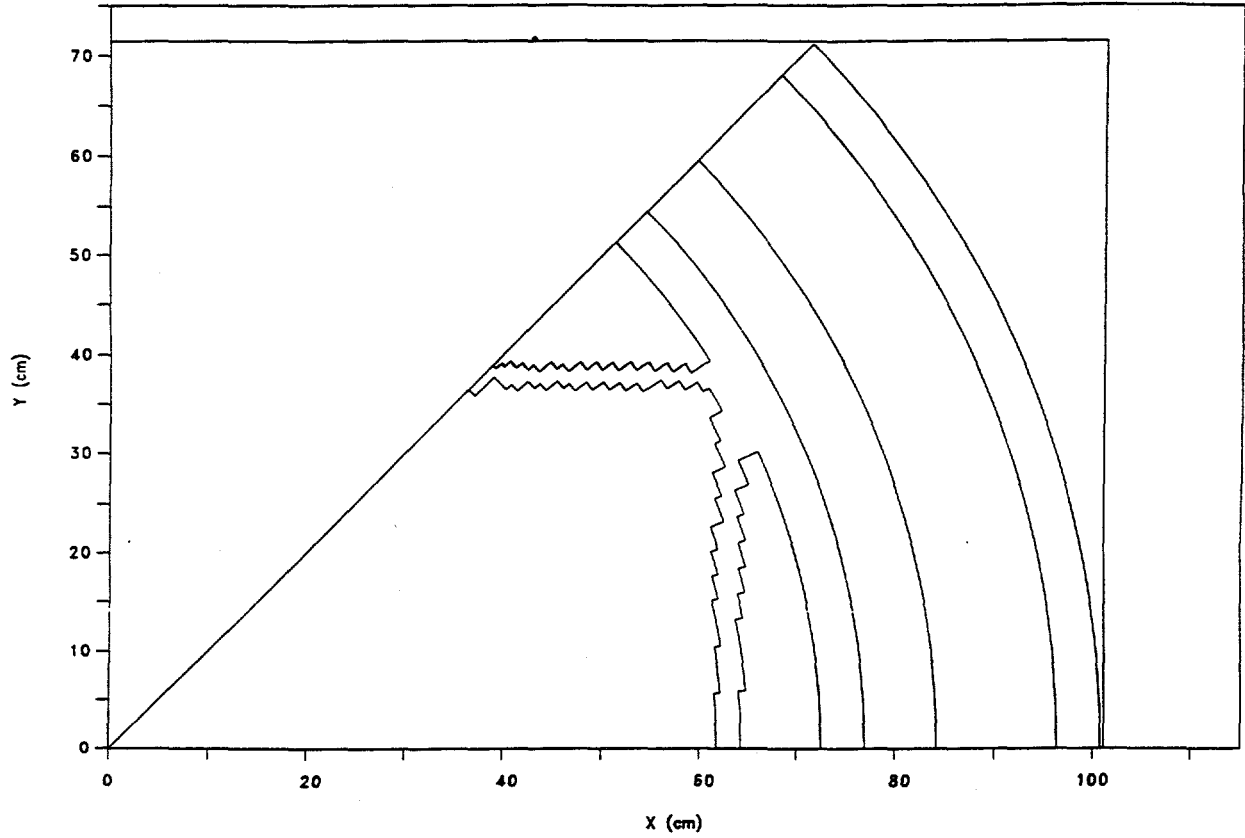


Fig. 4. The R- θ sample problem geometry.

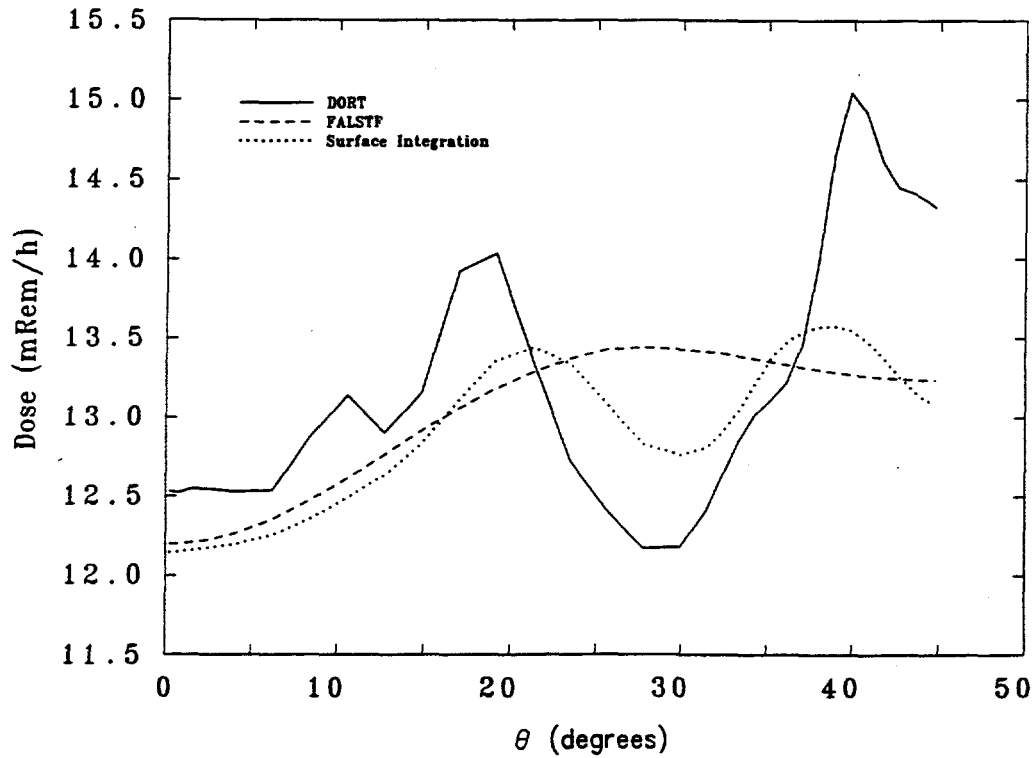


Fig. 5. Dose at 1 m from the surface.

7. REFERENCES

1. W. A. Rhoades and R. L. Childs, "The DORT Two-Dimensional Discrete Ordinates Code," *Nucl. Sci. Eng.* 99, 88-89 (May 1988).
2. F. R. Mynatt, F. J. Muckenthaler, and P. N. Stevens, *Development of a Two-Dimensional Discrete Ordinates Transport Theory for Radiation Shielding*, CTC-INF-952, Union Carbide Corp., Nucl. Div., Oak Ridge Natl. Lab. (August 1969).
3. G. I. Bell and S. Glasstone, *Nuclear Reactor Theory*, Van Nostrand Reinhold Co., New York, 1970.
4. B. L. Broadhead, M. C. Brady, and C. V. Parks, *Benchmark Shielding Calculations for the NEACRP Working Group on Shielding Assessment of Transportation Packages*, ORNL/CSD/TM-272, Martin Marietta Energy Systems, Inc., Oak Ridge Natl. Lab. (November 1990).
5. A. F. Avery and H. F. Locke, *NEACRP Comparison of Codes for the Radiation Protection Assessment of Transportation Packages. Solutions to Problems 1-4*, NEACRP-L-331, AEA Technology, Winfrith (March 1992).
6. J. S. Tang, "SAS4: A Monte Carlo Cask Shielding Analysis Module Using an Automated Biasing Procedure," Sect. S4 of *SCALE: A Modular Code System for Performing Standardized Computer Analyses for Licensing Evaluation*, NUREG/CR-0200, Rev. 4 (ORNL/NUREG/CSD-2/R4), Vols. I, II, and III (draft February 1990). Available from Radiation Shielding Information Center as CCC-545.
7. *SCALE: A Modular Code System for Performing Standardized Computer Analyses for Licensing Evaluation, Vols. I-III*, NUREG/CR-0200, Rev. 4 (ORNL/NUREG/CSD-2/R4), (April 1995). Available from Radiation Shielding Information Center as CCC-545.

APPENDIX A

THE VARSOR2D INTERFACE FILE

```
-----  
-  
- name:      varsor2d  
-  
- date:      29 nov 93  
-  
- purpose:   total source moments and associated interpretive data  
-  
- notes:     order of groups is by decreasing energy --  
-             neutrons, then photons.  
-  
-             i is the first -dimension index.  
-             j is the second-dimension index.  
-  
-             when im.gt.0, the mesh is a regular mesh with im cells in  
-             each row. ism=1.  
-  
-             when im.lt.0, the mesh is discontinuous. each row  
-             contains ims cells, where ims=imbis(iset(j)).  
-  
-             material component, izcomp, is the old 'dot-style' index.  
-  
-             mult=1 with 8-byte words; =2 with 4-byte words  
-----
```

```
-----  
- file structure:  
-  
- record type      present if  
- -----  
- file identification      always  
- file label               always  
- integer parameters      always  
- integer arrays          always  
- indexing arrays         always  
- real arrays              always  
-  
- cell zone identification      always  
- cell density factors         idfac=1  
-  
- .....do ig=1,igm  
- .   cell total cross section      always  
- .....enddo  
-  
- .....do ig=1,igm  
- .   .....do j=1,jm  
- .   cell total source moments      always  
- .   .....enddo  
- .....enddo  
-----
```

```
-----  
- file identification:  
-  
- hname, (huse(i),i=1,2),ivers  
-----
```

```

-   number of words= 4*mult
-
-   hname          file name          - (a8)
-   huse(i)        user file identification - (a8)
-   ivers          file version number  - (a8)
-----
-
- file label:
-
-   date,user,charge,case,time,(titl(i),i=1,9)
-
-   number of words= 14*mult
-
-   date           as provided by timer option 4 - (a8)
-   user           as provided by timer option 5 - (a8)
-   charge         as provided by timer option 6 - (a8)
-   case           as provided by timer option 7 - (a8)
-   time           as provided by timer option 8 - (a8)
-   titl(i)        title provided by user      - (a8)
-----
-
- integer parameters:
-
-   igm,im,jm,km,izm, neut,ism,jsm,imsism,jmsjms, jmskm,nconv
-   , (idum(n),n=1,9)
-
-   number of words= 25
-
-   igm            number of energy groups
-   im             maximum number of cells in any row
-   jm            number of rows
-   mtm           number of material cross section sets
-   izm           number of material zones
-
-   neut          last neutron group
-                 (igm if all neutrons, 0 if all photons)
-   ism           number of isets
-   imsjm         sum of ims over j=1,jm
-   imsism        sum of ims over is=1,ims
-   isctm         maximum order of cross section expansion
-
-   idfac         0=density factors not used; 1=used
-   ingeom        0=xz; 1=rz; 2=r-theta
-   ibl           left  boundary conditon
-   ibr           right boundary conditon
-   ibb           bottom boundary conditon
-
-   ibt           top   boundary conditon
-   idum          array set to 0
-----
-
- integer arrays:
-   (izcomp(iz),iz=1,izm), (iznrg(iz),iz=1,izm)
-   , (lmbig(ig),ig=1,igm)
-
-   number of words= izm+izm+igm
-
-   izcomp        material component by material zone
-   iznrg         edit region by material zone

```

- lmbig moment expansion by energy group
-

- indexing arrays:

- (imbis(is),is=1,ism), (iset(j),j=1,jm)
-
- number of words= ims+jm
-
- imbis number of cells in i-set is
- iset i-set assigned to row j
-

- real arrays:

- ((r(i,is),i=1,ims+1),is=1,ism), (z(j),j=1,jm)
- , (ener(ig),ig=1,igm),emin,eneut, (dumrl(i),i=1,8)
-
- number of words = imsism+ism+jm+1+igm+2+8
-
- r i-interval boundaries by i-set
- z j-interval boundaries by j
-
- ener top energy boundary of group ig
- emin bottom energy boundary of group igm
- eneut bottom energy boundary of group neut
- (0 if neut=0)
- dumrl array set to 0.
-

- cell zone identification:

- ((ijzn(i,j),i=1,ims),j=1,jm)
-
- number of words = imsjm
-
- ijzn material zone by cell
-

- cell density factors:

- ((dni(j,i),i=1,ims),j=1,jm)
-
- number of words = imsjm
-
- dni(j,i) cell density factors
-

```
- total cross section
-
-   (sig(mt), mt=1, mtm)
-
-   number of words = mtm
-
-   sig           total cross section
-
-----
```

```
-----
- source moments
-
-   ((sorm(i,l), i=1, ims), l=1, lms)
-
-   number of words = ims*lms
-
-   sorm           source by interval and moment index
-   ims           imbis(is) for is corresponding to j
-   lms           lmbig(ig)
-
-----
```

APPENDIX B

THE R-Z SAMPLE PROBLEM FALSTF OUTPUT

```
1$ array      3 entries read
2$ array      3 entries read

0t
/
1$$ /          fortran logical unit numbers
/
30 / ntdso - dort distributed source unit
/           default = 30
0 / ntf  - falstf detector flux output unit
/           default = 0 ; 0 means no effect
0 / ntzf - detector flux by dort zone output unit
/           default = 0 ; 0 means no effect
/
/
2$$ /          integer input variables
/
45 / ndet - number of detector locations
/           default = 1
0 / neut  - last neutron group ; 0 means all gamma
/           default read from ntdso
12 / noa  - number of angles for azimuthal integration
/           default = 12
/           should be multiple of 6
/

      information from ntdso
igm = 13 number of energy groups
im  = 39 number of radial intervals
jm  = 58 number of axial intervals
izm = 4 number of spatial zones
isctm= 3 order of legendre expansion of the
      scattering source
title=dort: oecd problem 1a ; falstf sample problem
date =12/13/93
time =13:57:16
```

```
words of storage required = 25937
words of storage available = 2000000
```

```
27* array      13 entries read
42* array      45 entries read
44* array      45 entries read
```

```
0t
```

dose factors by group (from 27** array)

1	3.95960E-06
2	3.46860E-06
3	3.01920E-06
4	2.62760E-06
5	2.20510E-06
6	1.83260E-06
7	1.52280E-06
8	1.17250E-06
9	8.75940E-07
10	6.30610E-07
11	3.83380E-07
12	2.66930E-07
13	9.34720E-07

s10
2.0 cm intervals

detector number	neutron dose	gamma dose	detector radius	detector z
1	0.00000E+00	4.88229E-03	0.00000E+00	2.67500E+02
2	0.00000E+00	4.22616E-03	4.00000E+00	2.67500E+02
3	0.00000E+00	4.05599E-03	8.00000E+00	2.67500E+02
4	0.00000E+00	4.00551E-03	1.20000E+01	2.67500E+02
5	0.00000E+00	3.94290E-03	1.60000E+01	2.67500E+02
6	0.00000E+00	3.79491E-03	2.00000E+01	2.67500E+02
7	0.00000E+00	3.54005E-03	2.40000E+01	2.67500E+02
8	0.00000E+00	3.08726E-03	2.80000E+01	2.67500E+02
9	0.00000E+00	2.58409E-03	3.20000E+01	2.67500E+02
10	0.00000E+00	2.19894E-03	3.60000E+01	2.67500E+02
11	0.00000E+00	2.08485E-03	4.00000E+01	2.67500E+02
12	0.00000E+00	1.14957E-03	0.00000E+00	3.67000E+02
13	0.00000E+00	1.14644E-03	4.00000E+00	3.67000E+02
14	0.00000E+00	1.13710E-03	8.00000E+00	3.67000E+02
15	0.00000E+00	1.12172E-03	1.20000E+01	3.67000E+02
16	0.00000E+00	1.10062E-03	1.60000E+01	3.67000E+02
17	0.00000E+00	1.07424E-03	2.00000E+01	3.67000E+02
18	0.00000E+00	1.04306E-03	2.40000E+01	3.67000E+02
19	0.00000E+00	1.00766E-03	2.80000E+01	3.67000E+02
20	0.00000E+00	9.68725E-04	3.20000E+01	3.67000E+02
21	0.00000E+00	9.27005E-04	3.60000E+01	3.67000E+02
22	0.00000E+00	8.82691E-04	4.00000E+01	3.67000E+02
23	0.00000E+00	4.35135E-04	0.00000E+00	4.67000E+02
24	0.00000E+00	4.34616E-04	4.00000E+00	4.67000E+02
25	0.00000E+00	4.33108E-04	8.00000E+00	4.67000E+02
26	0.00000E+00	4.30615E-04	1.20000E+01	4.67000E+02
27	0.00000E+00	4.27157E-04	1.60000E+01	4.67000E+02
28	0.00000E+00	4.22771E-04	2.00000E+01	4.67000E+02
29	0.00000E+00	4.17487E-04	2.40000E+01	4.67000E+02
30	0.00000E+00	4.11357E-04	2.80000E+01	4.67000E+02
31	0.00000E+00	4.04479E-04	3.20000E+01	4.67000E+02
32	0.00000E+00	3.96895E-04	3.60000E+01	4.67000E+02
33	0.00000E+00	3.88462E-04	4.00000E+01	4.67000E+02
34	0.00000E+00	2.22167E-04	0.00000E+00	5.67000E+02
35	0.00000E+00	2.22033E-04	4.00000E+00	5.67000E+02
36	0.00000E+00	2.21625E-04	8.00000E+00	5.67000E+02
37	0.00000E+00	2.20948E-04	1.20000E+01	5.67000E+02
38	0.00000E+00	2.20003E-04	1.60000E+01	5.67000E+02
39	0.00000E+00	2.18794E-04	2.00000E+01	5.67000E+02
40	0.00000E+00	2.17338E-04	2.40000E+01	5.67000E+02
41	0.00000E+00	2.15650E-04	2.80000E+01	5.67000E+02
42	0.00000E+00	2.13742E-04	3.20000E+01	5.67000E+02
43	0.00000E+00	2.11551E-04	3.60000E+01	5.67000E+02
44	0.00000E+00	2.09085E-04	4.00000E+01	5.67000E+02
45	0.00000E+00	2.40864E-05	0.00000E+00	1.26700E+03



INTERNAL DISTRIBUTION

- | | | | |
|--------|--------------------|--------|-----------------------------|
| 1. | Y. Azmy | 27. | C. V. Parks |
| 2. | J. M. Barnes | 28. | L. M. Petrie |
| 3. | S. M. Bowman | 29. | R. T. Primm |
| 4. | B. L. Broadhead | 30. | J. P. Renier |
| 5. | J. A. Bucholz | 31. | R. W. Roussin |
| 6-10. | R. L. Childs (5) | 32. | C. H. Shappert |
| 11. | M. D. DeHart | 33. | D. B. Simpson |
| 12. | M. B. Emmett | 34. | C. O. Slater |
| 13. | T. A. Gabriel | 35. | J. S. Tang |
| 14. | J. C. Gehin | 36. | R. M. Westfall |
| 15. | D. T. Ingersoll | 37. | L. R. Williams |
| 16. | J. O. Johnson | 38. | B. A. Worley |
| 17. | M. A. Kuliasha | 39-40. | Laboratory Records Dept. |
| 18. | L. C. Leal | 41. | Laboratory Records, ORNL-RC |
| 19. | R. A. Lillie | 42. | Y-12 Technical Library |
| 20. | J. B. Manneschildt | 43. | Central Research Library |
| 21-25. | L. F. Norris | | Document Reference Section |
| 26. | J. V. Pace | 44. | ORNL Patent Section |

EXTERNAL DISTRIBUTION

45. M. Bailey, U.S. Nuclear Regulatory Commission, Office of Nuclear Material Safeguards and Safety, IMNS STSB, MS 8 F5, Washington, DC 20555
46. W. Davis, TESS, B&W Fuel Co., MS 423, Suite 527, P.O. Box 98608, 101 Convention Center Drive, Las Vegas, NV 89109
- 47-49. T. Doering, TESS, B&W Fuel Co., MS 423, Suite 527, P.O. Box 98608, 101 Convention Center Drive, Las Vegas, NV 89109
50. L. Hassler, Babcock & Wilcox, P.O. Box 10935, Lynchburg, VA 24506-0935
51. D. Lancaster, 2650 Park Tower Drive, Suite 800, Vienna, VA 22180
52. D. Napolitano, Nuclear Assurance Corp., 655 Engineering Dr., Suite 200, Norcross, GA 30092
53. Office of Scientific and Technical Information, U.S. Department of Energy, P.O. Box 62, Oak Ridge, TN 37831
54. Office of the ORNL Site Manager, Department of Energy, Oak Ridge National Laboratory, P.O. Box 2008, Oak Ridge, TN 37831
55. M. Rahimi, 2650 Park Tower Drive, Suite 800, Vienna, VA 22180

56. D. A. Thomas, TESS, B&W Fuel Co., MS 423, Suite 527, P.O. Box 98608, 101 Convention Center Drive, Las Vegas, NV 89109
57. J. R. Thornton, Duke Engineering & Services, Inc., 2300 S. Tryon St., P.O. Box 1004, Charlotte, NC 28201-1004
58. B. White, U.S. Nuclear Regulatory Commission, Office of Nuclear Material Safety and Safeguards, IMNS, MS 8 F5, Washington, DC 20555
59. M. L. Williams, LSU Nuclear Science Center, Baton Rouge, LA 70803
60. C. J. Withee, U.S. Nuclear Regulatory Commission, Office of Nuclear Material Safety and Safeguards, MS 8 F5, Washington, DC 20555